Magneto-optical properties of MnBi and MnBiAl

R. F. Sabiryanov and S. S. Jaswal
Behlen Laboratory of Physics and Center for Materials Research and Analysis, University of Nebraska, Lincoln, Nebraska 68588-0111
(Received 4 April 1995; revised manuscript received 16 June 1995)

First-principle electronic structure calculations are used to describe the magneto-optical properties of MnBiAl alloys as a function of the Al concentration. The calculated Kerr rotation and ellipticity are in good agreement with the experimental data for MnBi. Due to lack of good structural information, the magneto-optical properties of MnBiAl are studied for Al as (a) an interstitial and (b) partially substituting for Bi. The Kerr rotation of MnBi degrades with interstitial Al but remains about the same for a small amount of substitutional Al. The latter result is in agreement with the experimental data. Thus, both theory and experiment are in agreement that Al does not improve the magneto-optical properties of MnBi.

I. INTRODUCTION

MnBi has received considerable attention since its favorable magneto-optical properties were recognized.[1] Recently, many attempts have been made to improve the properties of MnBi by varying the stoichiometry or by substitution. Earlier investigations usually gave the magnitude of Kerr rotation in the range 0.55–1.0°. Then a huge increase of the Kerr rotation up to 2.04° was reported by the addition of Al and Si to MnBi.[2] A maximum Kerr rotation was reported for the composition $Mn_{1.0}Bi_{0.8}Al_{0.5}Si_{2.5}$. The recent experimental data by Di *et al.* show similar large Kerr rotation both in homogeneous MnBi and MnBiAl alloys for concentration of Al up to 10%.[3,4] They also find that 14% Al concentration suppresses the Kerr rotation angle to zero degree. The results for MnBiAl films also suggest that Kerr rotation for $Mn_1Bi_{0.8}Al_{0.4}$ is similar to that in pure MnBi.[5]

The self-consistent spin-polarized band structure calculations for MnBi were performed by Coehoorn *et al.*[6,7] and the effect of spin-orbital interactions on the electronic structure has been studied by Jaswal *et al.*[5] We report here *ab-initio* investigation of the electronic structure and magneto-optical properties of MnBi alloys. We also consider the influence of Al on the magneto-optical properties of MnBi. Due to the lack of structural data we study both interstitial and substitutional (Bi-site) position of Al atoms in MnBiAl alloys.

II. COMPUTATIONAL PROCEDURE

We consider the direction of magnetization and the linearly polarized light to be normal to the interface between nonmagnetic and magnetic media (z direction). The rotation of the polarization direction and the ellipticity of the reflected light are called the Kerr effect. The left-handed $(-)$ and the right-handed $(+)$ components of the conductivity are given by

$$\sigma^{\pm}(\omega)=\sigma_{xx}(\omega)\pm i\sigma_{xy}(\omega), \tag{1}$$

where the conductivity tensor has the following form:

$$\begin{pmatrix} \sigma_{xx} & \sigma_{xy} & 0 \\ -\sigma_{xy} & \sigma_{xx} & 0 \\ 0 & 0 & \sigma_{zz} \end{pmatrix}. \tag{2}$$

For the linearly polarized light the complex Kerr rotation is given by[8]

$$\theta_k + i\,\eta_k = i\sqrt{\epsilon_0}\frac{\sqrt{\epsilon^+}-\sqrt{\epsilon^-}}{\sqrt{\epsilon^+}\sqrt{\epsilon^-}-\epsilon_0}, \tag{3}$$

where θ_k and η_k are the Kerr rotation and ellipticity, respectively and ϵ_0 and $\epsilon^{\pm}$ are the dielectric constants in nonmagnetic and magnetic media, respectively. $\epsilon^{\pm}$ is related to the $\sigma^{\pm}$ by

$$\epsilon^{\pm}=1+\frac{4\pi}{\omega}i\sigma^{\pm}. \tag{4}$$

The magneto-optic effect is determined by the off-diagonal component of the conductivity tensor. This anisotropy of the motion of an electron is determined, in the absence of external magnetic field, by the spin-orbital interactions.

The conductivity tensor, as a function of the frequency ω for interband transitions in the random phase approximation without allowance for the local field effects, is given by[9]

$$\sigma_{\alpha\beta}(\omega)=\frac{1}{\pi}\int d\omega' I(\omega')\left(\frac{1}{\omega-\omega'+i/\tau}+\frac{1}{\omega+\omega'+i/\tau}\right), \tag{5}$$

where τ is the relaxation time and the expression for $I(\omega)$ is given below.

$$I(\omega)=\frac{\pi e^2}{2\omega}\sum_{\mathbf{k}\lambda\neq\lambda'}\delta(h\omega-E_{\lambda\lambda'}(\mathbf{k}))\{\theta(E_\lambda(\mathbf{k})-E_F) - \theta(E_{\lambda'}(\mathbf{k})-E_F)\}\mathrm{Im}[j_\alpha^{\lambda\lambda'}(\mathbf{k})j_\beta^{\lambda\lambda'}(\mathbf{k})], \tag{6}$$

where $E_{\lambda\lambda'}(\mathbf{k})$ is the difference in the energies of the one-electron states $|\mathbf{k}\lambda\rangle$ and $|\mathbf{k}\lambda'\rangle$, the Fermi function has been

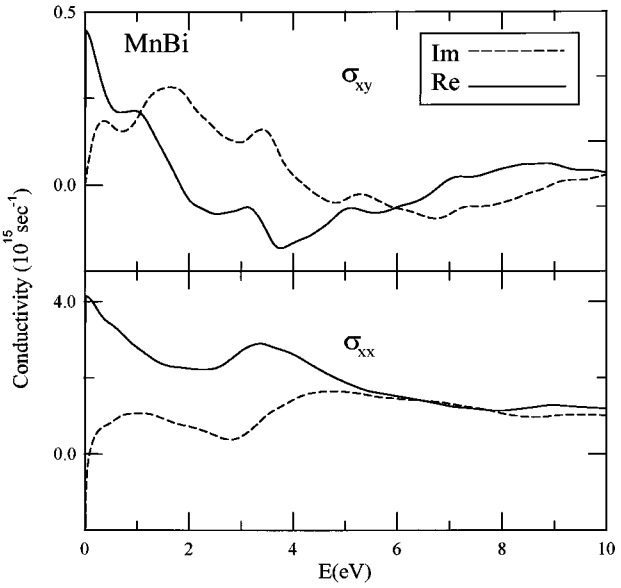

FIG. 1. Real and imaginary parts of σ^{xx} and σ^{xy} of MnBi.

replaced with the step function θ, and the matrix element of the current density operator without the spin-orbit term is given by

$$j_\alpha^{\lambda\lambda'}(\mathbf{k}) = \langle \mathbf{k}\lambda | \hat{p}_\alpha | \mathbf{k}\lambda' \rangle. \tag{7}$$

We use the linear-muffin-tin-orbitals (LMTO) method[10] in the near orthogonal representation to perform spin-polarized self-consistent electronic structure calculations with the scalar-relativistic and spin-orbit correction terms included in the Hamiltonian. The local-density LMTO calculations are based on the atomic sphere approximation corrected to first order by the combined correction term. The details of the calculation of matrix elements of the current density operator in terms of LMTO method are given in Ref. 11. The linear tetrahedron method[12,13] is used to calculate the real and imaginary parts of σ simultaneously. We use the procedure developed in Ref. 14 to calculate Green function in the complex plane (some other papers dealing with similar procedures are Refs. 15 and 16). When the Fermi surface intersects a tetrahedron, the matrix elements are linearly interpolated and the integration is carried out up to the Fermi energy only. Oppeneer *et al.*[17] have used the linear tetrahedron method to calculate the real and imaginary parts of the conductivity tensor simultaneously. This procedure avoids the numerical errors that can arise in Kramers-Kronig transformation.

The intraband contribution to the diagonal component of conductivity tensor is given by Drude formula

$$\sigma(\omega) = \frac{\sigma_0}{1 - i\omega\tau_D}, \tag{8}$$

where σ_0 is the dc conductivity and τ_D is the intraband relaxation time. τ_D is calculated from the computed plasma frequency ω_p and the experimental value of σ_0. In single frequency approach the ω_p is given by[18]

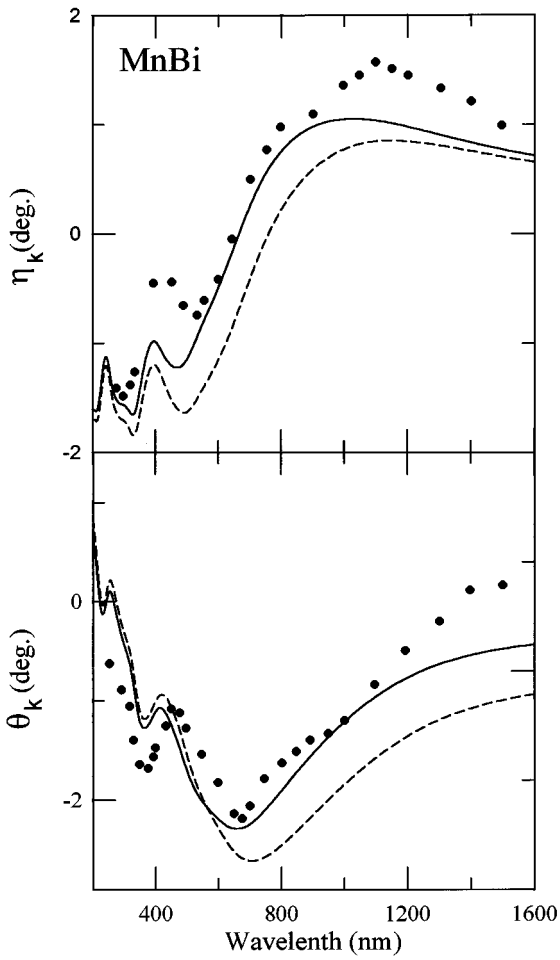

FIG. 2. Kerr rotation (θ_k) and ellipticity (η_k) for MnBi. Dots represent the experimental data at 85 K from Ref. 4. Full line gives the results with the interband and intraband contributions while the dashed line corresponds to interband contribution only.

$$\omega_p^2 = \frac{4\pi e^2}{\Omega} \sum_{\mathbf{k}\lambda} |\mathbf{V}_{\mathbf{k}\lambda}|^2 \delta(E_{\mathbf{k}\lambda} - E_F), \tag{9}$$

where Ω is the volume of the primitive cell and

$$\mathbf{V}_{\mathbf{k}\lambda} = \langle \mathbf{k}\lambda | \nabla | \mathbf{k}\lambda \rangle \tag{10}$$

is the mean velocity of an electron in state $|\mathbf{k}\lambda\rangle$ and E_F is the Fermi energy.

III. RESULTS AND DISCUSSION

Stable MnBi alloy has hexagonal symmetry with four atoms per unit cell (space group $P6_3/mmc$, $a = 4.285$ Å, $c = 6.113$ Å).[19] The Wigner-Seitz radii for Mn and Bi are 1.633 Å and 1.1924 Å, respectively. The relativistic spin-polarized self-consistent calculations of the electronic structure have been carried out for 364 k points in the irreductible part of the Brillouin zone. The conductivity tensor calculated with this electronic structure is shown in Fig. 1. The interband contributions are based on a Lorenzian broadening with a lifetime parameter $\hbar/\tau = 0.35$ eV to take into account quasiparticle lifetime effects. The relaxation time τ_D for intraband contribution is estimated from calculated plasma fre-

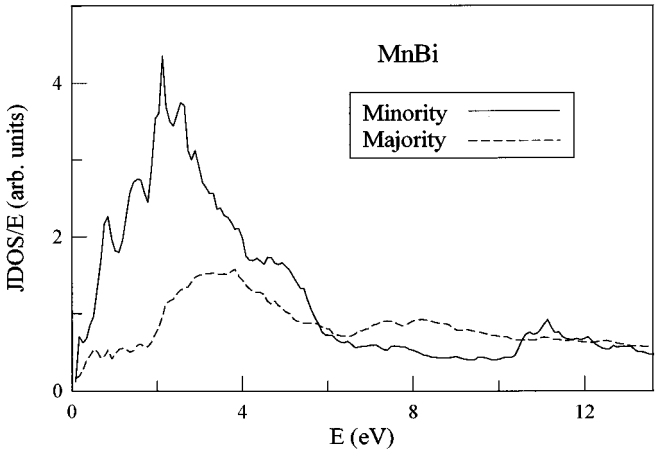

FIG. 3. Spin-resolved joint density of states divided by the energy E for MnBi.

quency and experimental dc conductivity[20] giving $\hbar/\tau_D=0.22$ eV. We see from Fig. 1 that σ_{xy} on the average is lower than σ_{xx} by about a factor of 10. The calculated σ and the values of ϵ_0 from Ref. 21 for the glass substrate are used to calculate the Kerr rotation for MnBi studied experimentally by Di.[4] The calculated spectra are compared with the experimental data in Fig. 2 and the two results are in good agreement with each other. The Kerr rotation angle has two main peaks: calculated $\theta_k=2.3°$ around 630 nm ($\approx$2 eV) and $\theta_k=1.3°$ around 380 nm ($\approx$3.3 eV). Figure 2 also shows the Kerr rotation without the intraband contribution which is appreciable at longer wavelengths but become negligible below 600 nm. The intraband contribution to only the diagonal component of σ has been included in all Kerr rotation calculations.

The Kerr rotation is a fairly complex function of σ_{xx} and σ_{xy} as given by Eq. (3) but σ_{xy} must be nonzero to get finite Kerr rotation. As mentioned above the intraband contribution is significant below 2 eV but is negligible above this energy. To correlate the calculated Kerr rotation to interband transitions we have plotted the joint density of states (JDOS) divided by energy E in Fig. 3. The minority spin JDOS has a large peak around 2 eV which arises from a modest peak around 1.4 eV below E_F and a large peak at 0.6 eV above E_F in the density of states (DOS) of MnBi shown in Fig. 4. The 2 eV peak in JDOS makes the major contribution to the largest Kerr rotation angle in Fig. 1 with transitions primarily from Bi $6p$ states around 1.4 eV below E_F to Mn $3d$ states around 0.6 eV above E_F. The majority spin JDOS has a small broad peak around 3.3 eV which arises from a large peak around that energy below E_F and a fairly flat DOS above E_F as shown in Fig. 4. This peak in JDOS is responsible for the second peak in Kerr-rotation angle around 3.3 eV with transitions primarily from Mn $3d$ states below E_F to Bi $6p$ state above E_F. The three main peaks in Im σ_{xy} in Fig. 1 correlate well that the corresponding features in the combined JDOS implying appreciable MO matrix elements between Bi $6p$ and Mn $3d$ states mentioned above.

The bands in the symmetry directions are plotted in Fig. 5 which clearly show the flat bands near the E_F responsible for the peaks in DOS mentioned above. Since the spin-orbit interactions mix the majority and minority states, the bands

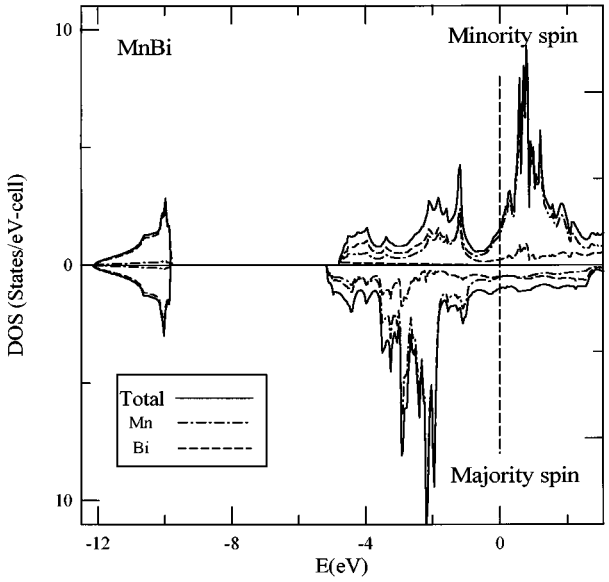

FIG. 4. Spin-polarized total and projected density of states of MnBi. The zero on the energy axis corresponds to the Fermi energy.

plotted in Fig. 5 are without the spin-orbit term in the Hamiltonian. This approximation does not have any effect on the present discussion due to the fact that the spin-orbit contributions are small. The bands have been truncated at 6 eV above the Fermi energy because they do not contribute to the Kerr spectrum of experimental interest.

Several attempts have been made to improve magneto-optical properties of MnBi using various doping elements

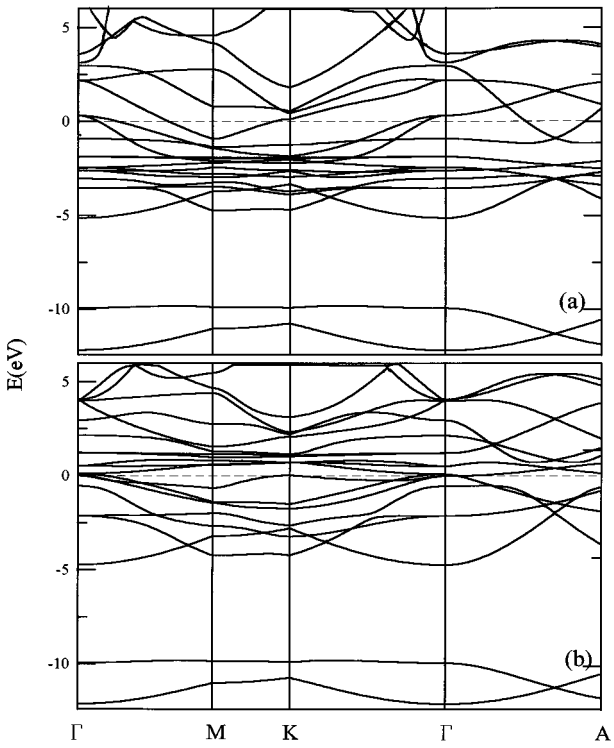

FIG. 5. Scalar-relativistic band structure for MnBi: (a) majority spin and (b) minority spin. The zero on the energy axis corresponds to the Fermi energy.

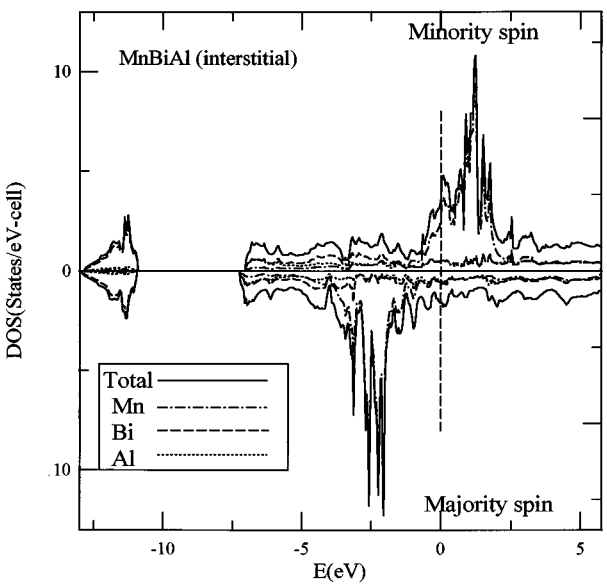

FIG. 6. Spin-polarized total and projected density of states of MnBiAl. Al is located in interstitial d sites. The zero on the energy axis corresponds to the Fermi energy.

such as Al. There is a lack of structural information on MnBiAl necessary for first-principle calculations. It is now well known that the c lattice constant of MnBi remains unchanged with the addition of Al. However, the effect of Al on the a lattice constant of MnBi is unclear. Di claims that a lattice constant also remains unchanged with the addition of Al.[4] He also found that β-MnBi phase grows preferentially for Al concentration larger than 10%. The location of Al in MnBiAl is also not known. Jaswal *et al.* considered interstitial site for Al.[5] They had to increase the a lattice constant by 15% to allow for a reasonable distance between the neighboring Bi and Al atoms. Density of states for this system is presented in Fig. 6. The main change is the absence of the peak in the minority spin DOS below E_F that is responsible for the major contribution to the Kerr rotation in MnBi. Thus, despite the large magnetic moment on Mn and considerable orbital moment (see Table I), the Kerr rotation angle is more than three times smaller than that in MnBi at the same frequency (Fig. 7). Most of the experimental data, however, suggest the Kerr rotation is not very sensitive to the Al doping.

Since the Bi concentration in MnBiAl is below that of a stoichiometric compound and Al radius is comparable to that of Bi, a partial substitution of Al for Bi is a possible structural model for MnBiAl. This is a more plausible model if the lattice constants remain unchanged with the addition of Al as claimed by Di. We consider two compositions, $MnBi_{0.75}Al_{0.25}$ and $MnBi_{0.5}Al_{0.5}$. The DOS for these modifications are more similar to that of MnBi than that of the interstitial model (Fig. 8). As a result, the Kerr rotation decreases on the average by ~10% for the first and ~40% for the second composition compared to that of MnBi (Fig. 7). For a good overall agreement with structural and magneto-optical data, the present calculations suggest that Al substitutes for about 13% Bi in MnBi ($MnBi_{0.75}Al_{0.25}$).

The possible locations of Al in MnBiAl can also be considered from the point of view of stability of the system with

TABLE I. The spin (M_s) and orbital (M_o) moments of Mn, Bi, and Al in μ_B in various MnBiAl compounds.

Composition	Atom	M_s	M_o
MnBi	Mn	3.60	0.082
	Bi	−0.11	−0.036
MnBiAl	Mn	4.02	−0.034
(interstitial)	Bi	0.04	0.005
	Al	0.01	0.004
$MnBi_{0.75}Al_{0.25}$	Mn	3.61	−0.010
(substitutional)	Bi	−0.12	−0.047
	Al	−0.29	0.045
$MnBi_{0.5}Al_{0.5}$	Mn	3.53	−0.068
(substitutional)	Bi	−0.13	−0.058
	Al	−0.26	0.050

doping. It is a difficult problem. We consider cohesive energy, E_{coh}, as one of the criteria for relative stability of the system with different locations of the doping element. Calculated cohesive energies for four elementary cells show that

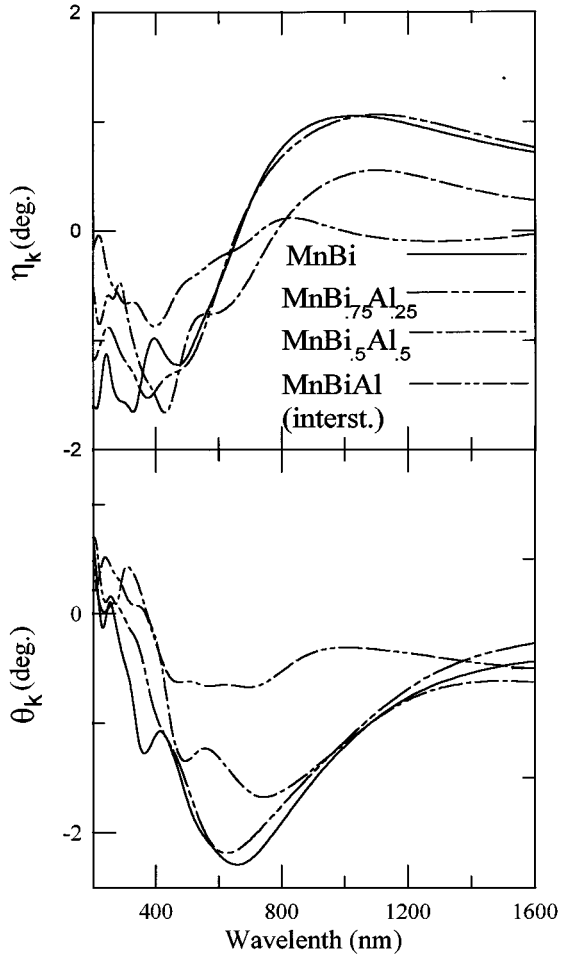

FIG. 7. Kerr rotation, θ_k, and ellipticity, η_k, for different MnBi-Al alloys.

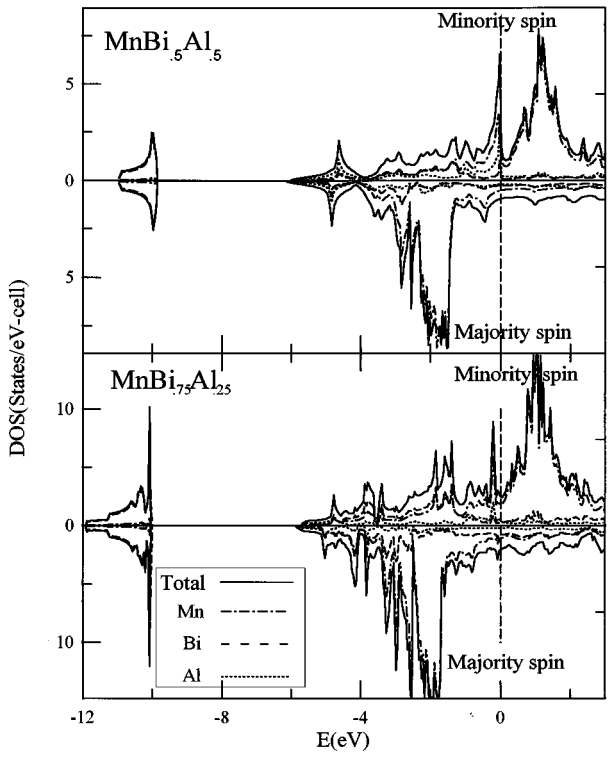

FIG. 8. Spin-polarized total and projected density of states of $MnBi_{0.75}Al_{0.25}$ and $MnBi_{0.5}Al_{05}$, where Al is substituting for Bi. The zero on the energy axis corresponds to the Fermi energy.

the two positions of Al considered here lower the absolute value of E_{coh}. Interstitial position is the most unfavorable location (21% decrease in $|E_{\mathrm{coh}}|$). Each additional Al in substitutional position decreases $|E_{\mathrm{coh}}|$ by 4.2%. Thus, cohesive energy calculations also support the substitutional model with a small amount of Al substituting for Bi in MnBi.

Finally, for the sake of completeness we list the spin and orbital magnetic moments in Table I. Mn induces small spin moments on the nonmagnetic atoms (Bi,Al) through overlap exchange interactions. A ferromagnetic induced moment means that the nonmagnetic atom has stronger exchange hybridization with the majority spin states of Mn. The opposite holds for the antiferromagnetic induced moment. The signs of the moments vary in different alloys depending on the local geometry of the nonmagnetic moment. We are not able to make a similar qualitative statement to explain the sign changes of the small orbital moments of different atoms. However, it is clear from Table I that a larger total orbital moment does not always imply a larger Kerr rotation.

IV. CONCLUSION

The results of the present calculations show strong dependence of magneto-optical properties on the peculiarities of hybridization in MnBi alloys. The calculated Kerr effect results agree reasonably well with the experimental data for MnBi. When compared with the experimental results that the addition of Al to MnBi has very little effect on the lattice constant and Kerr rotation, the present calculations suggest that Al substitutes for about 13% of the Bi sites in MnBi. Perhaps the rest of the Al ends up at the grain boundaries. Additional structural studies might shed more light on the locations of Al atoms in the MnBiAl system.

ACKNOWLEDGMENTS

We are grateful to Dr. Antropov and Professor Harmon of Iowa State University for helpful interactions at the beginning of this work. We thank Randall Victora for reminding us to include the substrate effect on the Kerr rotation. We are indebted to Roger Kirby, David Sellmyer, and Kurt Wierman for many valuable discussions. This work was supported by the National Science Foundation under Grant No. OSR-9255225. We are thankful to the Center for Material Research and Analysis, Center for Communication and Information Science of the University of Nebraska, and the National Supercomputing Center at Cornell University for the computational facilities.

[1] H. J. Williams, R. C. Sherwood, F. G. Foster, and E. M. Kelley, J. Appl. Phys. **28**, 1181 (1957).
[2] Y. J. Wang, J. Magn. Magn. Mater. **84**, 39 (1990).
[3] C. Q. Di, S. Iwata, S. Tsunashima, and S. Uchiyama, J. Magn. Magn. Mater. **104-107**, 1023 (1992).
[4] C. Q. Di, Ph.D. thesis, 1992.
[5] S. S. Jaswal, J. X. Shen, R. D. Kirby, and D. J. Sellmyer, J. Appl. Phys. **75**, 6346 (1994).
[6] R. Coehoorn and R. A. de Groot, J. Phys. F **15**, 2135 (1985).
[7] R. Coehoorn, C. Haas, and R. A. de Groot, Phys. Rev. B **31**, 1980 (1985).
[8] A. V. Sokolov, *Optical Properties of Metals* (Elsevier, New York, 1967).
[9] C. S. Wang and J. Callaway, Phys. Rev. B **9**, 4897 (1974).
[10] O. K. Andersen, Phys. Rev. B **12**, 3060 (1975).
[11] Yu. A. Uspenskii and S. V. Khalilov, Sov. Phys. JETP **68**, 588 (1989); Yu. A. Uspenskii, F. G. Maksimov, S. N. Rashkeev, and I. I. Mazin, Z. Phys. B **53**, 263 (1983).
[12] O. Jepsen and O. K. Andersen, Solid State Commun. **9**, 1763 (1971).
[13] G. Lehmann and M. Taut, Phys. Status Solidi B **54**, 469 (1972).
[14] Ph. Lambin and J. P. Vigneron, Phys. Rev. B **29**, 3430 (1984).
[15] P. T. Coleridge, J. Molenaar, and A. Lodder, J. Phys. C **15**, 6943 (1982).
[16] P. M. Oppeneer and A. Lodder, J. Phys. F. **17**, 1885 (1987).
[17] P. M. Oppeneer, T. Maurer, J. Sticht, and J. Kübler, Phys. Rev. B **45**, 10 924 (1992).
[18] I. I. Mazin, Ye. G. Maksimov, S. N. Rashkeyev, and Yu. A. Uspenskii, in *Metal Optics and Superconductivity*, edited by A. I. Golovashkin (Nova Science, New York, 1989), p. 1.
[19] H. Göbel, E. Wolfgang, and H. Harms, Phys. Status Solidi A **34a**, 553 (1976).
[20] D. Chen and Y. Gondo, J. Appl. Phys. **35**, 1024 (1964); D. Chen, Y. Gondo, and M. D. Blue, *ibid.* **36**, 1261 (1965).
[21] H. R. Philipp, in *Handbook of Optical Constants of Solids*, edited by E. D. Palik (Academic, New York, 1985), p. 749.